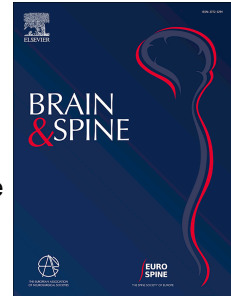


Journal Pre-proof

Increased variance in second electrode accuracy during deep brain stimulation and its relationship to pneumocephalus, brain shift, and clinical outcomes: A retrospective cohort study

M.G. Hart, M. Posa, P.C. Buttery, R.C. Morris



PII: S2772-5294(22)00034-0

DOI: <https://doi.org/10.1016/j.bas.2022.100893>

Reference: BAS 100893

To appear in: *Brain and Spine*

Received Date: 6 March 2022

Revised Date: 12 April 2022

Accepted Date: 28 April 2022

Please cite this article as: Hart, M.G., Posa, M., Buttery, P.C., Morris, R.C., Increased variance in second electrode accuracy during deep brain stimulation and its relationship to pneumocephalus, brain shift, and clinical outcomes: A retrospective cohort study, *Brain and Spine* (2022), doi: <https://doi.org/10.1016/j.bas.2022.100893>.

This is a PDF file of an article that has undergone enhancements after acceptance, such as the addition of a cover page and metadata, and formatting for readability, but it is not yet the definitive version of record. This version will undergo additional copyediting, typesetting and review before it is published in its final form, but we are providing this version to give early visibility of the article. Please note that, during the production process, errors may be discovered which could affect the content, and all legal disclaimers that apply to the journal pertain.

© 2022 Published by Elsevier B.V. on behalf of EUROSPINE, the Spine Society of Europe, EANS, the European Association of Neurosurgical Societies.

Increased variance in second electrode accuracy during deep brain stimulation and its relationship to pneumocephalus, brain shift, and clinical outcomes: a retrospective cohort study.

Hart MG¹, Posa M², Buttery PC³, Morris RC²

Affiliations

¹St George's University of London, Cranmer Terrace, London, SW17 0RE

²Department of neurosurgery, Addenbrooke's hospital, Cambridge, UK, CB2 0QQ

²Department of neurology, Addenbrooke's hospital, Cambridge, UK, CB2 0QQ

Corresponding Author

St George's University of London

Cranmer Terrace

London

SW17 0RE

Telephone: +44 (0) 781 008 0007

Email: mhart@sgul.ac.uk

Keywords: globus pallidus internus; magnetic resonance imaging; Parkinson's disease; subthalamic nucleus.

1 INTRODUCTION

2

3 Deep brain stimulation for Parkinson's disease is an effective treatment supported by
4 evidence from randomised controlled trials[1–5] and is now established in routine clinical
5 practice internationally. Despite the ubiquity and success of the procedure, methods for
6 appraisal of electrode accuracy – a key surgical outcome variable[6–9] – have not yet been
7 formalised. Failure to appreciate electrode accuracy may lead to excessive revision rates,
8 unsatisfactory clinical outcomes, and an inability to effectively appraise surgical results.

9

10 Placement of electrodes has historically relied on microelectrode recordings (MER) and
11 intraoperative macrostimulation during awake surgery[10]. More recently, image-guided
12 surgery under general anaesthesia without MER has been developed for reasons of efficiency,
13 patient comfort, and safety[11–14]. Methods for appraising electrode accuracy with either
14 technique are usually based on imaging, and while commercial and open-source software is
15 available for this purpose[15–21], reports of applications of these methods in routine clinical
16 practice are few.

17

18 Our aim was to test the applicability of image-based electrode localisation, specifically using
19 the open-source Lead-DBS toolbox[17,21], in routine clinical practice. In particular, we
20 wished to test the ability to interrogate the accuracy of our own deep brain stimulation
21 practice for Parkinson's disease using a direct targeting, MRI guided, and CT verified
22 technique under general anaesthesia. We hypothesised that the volume of the target nucleus
23 that was stimulated would correspond most strongly with motor outcomes. Furthermore, we
24 hypothesised that inaccuracy would be related to well-known variables, namely

1 pneumocephalus, intraoperative brain shift, and whether the electrode was inserted first or
2 second.

3

4 **MATERIALS AND METHODS**

5

6 **Patients**

7 A retrospective cohort study was performed of a consecutive series of patients with
8 Parkinson's disease who underwent deep brain stimulation of either the GPi or STN between
9 2016 and 2019. Patient selection for deep brain stimulation was performed in a multi-
10 disciplinary setting according to national commissioning criteria[22,23]. Targeting of the
11 subthalamic nucleus (STN) or globus pallidus internus (GPi) was based on individual
12 treatment goals as part of a multidisciplinary team assessment. Baseline patient details are
13 presented in table 1. Institutional ethical approval was granted as a review of service study.

14

15 **Surgical Procedure**

16 Surgery was performed as a single stage procedure under general anaesthesia with
17 implantation of electrodes manufactured by: St Jude/Abbott (Abbott Laboratories, Lake
18 Bluff, Illinois, USA: 6147 non-directional electrode with Libra PC system, or 6170
19 directional electrode with Infinity system), Medtronic (Medtronic Inc, Dublin, Eire: 3389
20 electrode with Activa PC system), or; Boston (Boston Scientific, Marlborough, Mass, USA:
21 Cartesia directional electrode and Vercise PC or Gevia system). Planning was performed
22 using StealthStation® S7™ (Medtronic Inc, Dublin, Eire) FrameLink® software. Direct
23 targeting was performed based on pre-operative 3 Tesla MRI data (magnetization-prepared
24 rapid-acquisition gradient-echo (MPRAGE) volumetric STEALTH sequences, proton density
25 (PD) sequences for the GPi, and susceptibility-weighted imaging (SWI) sequences for the

1 STN. Targets were planned to be based in the centre of the motor component of the nucleus.
2 A Leksell frame (Elekta AB, Stockholm, Sweden) was used in combination with pre-
3 operative and post-operative volumetric CT imaging for trajectory planning and verification,
4 respectively. If post-operative CT imaging demonstrated satisfactory appearances the
5 implantable pulse generator was placed during the same general anaesthetic. In all cases the
6 left hemisphere was implanted first.

7

8 **Image Registration, Electrode Reconstruction, and Calculation of Volume of Activated** 9 **Tissue (VAT)**

10 Image processing was performed using the Lead-DBS toolbox [17,21] (figure 1A).
11 Registration of the post-operative CT image to the standard space template of the Montreal
12 Neurological Institute (MNI152) was performed using Advanced Normalization Tools
13 (ANTs)[24,25]. Specifically, post-operative CT images were linearly registered to the pre-
14 operative T1-weighted MPRAGE image which in turn was registered to the ICBM152 2009b
15 template with non-linear diffeomorphic warping. Brain shift correction of subcortical
16 structures was performed using linear registration of an additional subcortical mask[26].

17

18 Electrodes were reconstructed based on the post-operative CT images using a combination of
19 PaCER[20] algorithm or if this failed TRA/CORE[17,21]. Subsequently manual refinement
20 was performed to align the electrode model with the imaging artefact on the corresponding
21 CT image.

22

23 Volume of Activated Tissue (VAT) reconstructions were performed using a finite element
24 model implemented in Lead-DBS[17,21]. A tetrahedral mesh was constructed based on a
25 four-compartment model comprising grey matter, white matter, and electrode (conducting

1 and non-conducting) components. Conductivity values were set according to standard
2 parameters then the VAT was binarised at a threshold of 0.2 Volts/mm. Finally, electrode
3 locations and VATs were visualised on the DISTAL atlas[27].

4

5 **Definition of Accuracy**

6 Electrode accuracy was defined as the shortest distance between any electrode contact and
7 the boundary of the target region (either main nucleus or motor subnucleus) (figure 1B). This
8 was defined in both the 2D plane for target plots and in terms of 3D Euclidean distance.

9 Electrode variance was defined as the distance in 3D Euclidean co-ordinates from the centre
10 of gravity of the target in question (either the main nucleus or motor subnucleus).

11

12 **Computation of Brain shift and Pneumocephalus**

13 Brain shift is believed to occur after durotomy and results in a complex and likely nonlinear
14 displacement of the brain that is poorly defined. This can result in significant difficulties in
15 registration between images as nonlinear transforms can impact on electrode localisation
16 robustness. Subsequently, one of the most well-developed methods to account for this relies
17 upon using layered linear transforms to subcortical regions of interest ([26]). We quantified
18 this approach by summing the resultant transformation matrix. Additionally, we localised
19 electrodes both with and without this approach to assess the difference it made to accuracy.

20 Pneumocephalus is typically related to durotomy and believed to be associated with brain
21 shift. We quantified the degree of pneumocephalus by using an MNI space brain mask which
22 defined pneumocephalus as the difference between this as the expected brain volume and the
23 actual extracted brain volume (figure 1C).

24

25 **Outcome Assessment**

1 Programming commenced at approximately 6 weeks following surgery and was led by a
2 consultant neurologist with a specialist interest in movement disorders in combination with a
3 specialist nurse. Initial programming commenced with a pulse width of $60\mu\text{s}$ and a frequency
4 of 130Hz. Outcome variables were recorded by a consultant neurologist in combination with
5 a specialist nurse at 12 months following surgery. Outcome measures included: body weight
6 (in kilograms); UPDRS 3; UPDRS 4; levodopa equivalent daily dose (LEDD); and PDQ39.

7

8 **Statistical Analysis**

9 Groups were analysed according to hemisphere (with the second electrode to be implanted
10 being in the right hemisphere), nucleus (GPi or STN), and target (main nucleus or motor
11 subnucleus). Distances from the electrode to, and overlap of the VAT with, the corresponding
12 nucleus and specific component of the nucleus were calculated. All values are expressed as
13 mean \pm 2 standard deviations (SD). Raincloud plots were generated to display raw data, box
14 plots, and half-violin plots of the data distribution ([28]).

15

16 Differences in continuous variables were performed with paired t-tests (dual groups) or
17 Analysis of Variance (ANOVA, multiple groups). Statistical dependencies between
18 continuous variables were analysed with Pearson's correlation. A general linear model was
19 fitted on clinical outcomes, electrode accuracy, and VAT's. Significance was set at $p < 0.05$
20 with corrections for multiple comparisons using the Bonferroni method. All analyses were
21 performed in MATLAB (version 9.7.0 (R2021a), Natick, Massachusetts: The MathWorks
22 Inc.) using open-source code (<https://github.com/jazzmanmike/DBS/>).

23

24 **RESULTS**

25

1 **Cohort Characteristics**

2 In total 38 participants met the inclusion criteria. Baseline clinical and demographic data of
3 the cohort are presented in Table 1. The only clinical adverse events were a device infection
4 that required system explantation and tethering of an implantable pulse generator managed
5 with revision surgery.

7 **Image Processing**

8 Overall, 30 out of 38 (79%) participants successfully completed the image processing
9 pipeline (supplementary figure 1). Reasons for exclusion from analysis included registration
10 failure (post-op CT to pre-op MRI, 6 participants) and failure of VAT construction (2
11 participants). Correction for brain shift with subcortical refine methodology was utilised in all
12 cases. Electrode reconstructions were performed primarily with PaCER, or TRA/CORE if
13 this was not possible (15 participants each).

15 **Clinical Outcomes**

16 Changes in clinical outcomes post-operatively are presented in figure 2 and table 2. In the
17 overall cohort, statistically significant improvements were demonstrated for UPDRS 3,
18 UPDRS 4, LEDD, and PDQ39. Stimulation of the STN compared with the GPi resulted in a
19 significantly greater reduction in LEDD (55% decrease versus 2% increase respectively,
20 $p < 0.001$) but otherwise there were no differences in outcomes. Finally, all the described
21 clinical outcomes were independent and did not demonstrate significant covariance
22 (supplementary figure 2: maximal R^2 0.13, $p = 0.12$).

24 **Electrode Accuracy**

1 Overall electrode accuracy was $0.22 \pm 0.4\text{mm}$ for all electrodes to the main nucleus with 9
2 (12%) outliers but only 3 (4%) electrodes out with 2mm from the intended target (figures 3
3 and 4). For GPi stimulation, electrodes were a mean of $0.26 \pm 0.43\text{mm}$ from the main
4 nucleus, and $0.80 \pm 0.97\text{mm}$ from the GPi motor nucleus. Overall, 17 out of 20 electrodes
5 were within 2mm of the main nucleus. For STN stimulation, electrodes were a mean of
6 0.14mm (SD 0.28) from the main nucleus, and 0.27mm (SD 0.52) from the STN motor
7 nucleus. Overall, all 40 electrodes were within 2mm of the main nucleus.

8
9 Nucleus (GPi or STN) affected accuracy with lower accuracy for electrodes in the GPi than
10 the STN ($0.43 \pm 0.62\text{mm}$ versus $0.11 \pm 0.12\text{mm}$, $p = 0.002$). There was no systematic co-
11 variance in accuracy between hemispheres ($r = 0.12$, $R^2 = 0.01$, $p = 0.52$). However, the
12 second electrode implanted (i.e. that in the right hemisphere) was less accurate than the first
13 electrode implanted ($0.09 \pm 0.03\text{mm}$ versus $0.34 \pm 0.53\text{mm}$, $p = 0.01$).

14
15 To determine which clinical scenario (GPi versus STN, main nucleus versus motor
16 subnucleus, right versus left side) accuracy is most likely to be affected, a systematic analysis
17 is presented in supplementary figure 3. Concordant with the main findings above, variance in
18 accuracy was most prominent in the right GPi (group F-stat = 9.68, $df = 7$, $p < 0.01$; GPi right
19 $t_{\text{stat}} = -2.9$, $df = 18$, $p = 0.01$). Accuracy did not vary depending on whether the target
20 reference was chosen to be the main nucleus or motor sub-nucleus ($t_{\text{stat}} = -1.1$, $df = 118$, $p =$
21 0.27).

22 23 **Systematic Variance in Accuracy**

24 Target plots of accuracy per nucleus, hemisphere, and target are presented in figure 5 to
25 determine if variation in accuracy occurred predominantly in any single Cartesian (XYZ)

1 dimension. Variance occurred predominantly in the X-dimension in the right hemisphere and
2 was consistent across nucleus (STN versus GPi) and target (overall nucleus versus motor sub-
3 nucleus) (supplementary figure 4). Utilisation of subcortical refine methodology (as an
4 adjustment for brain shift) did not affect accuracy in any single dimension.

5

6 **Relationship of Accuracy to Pneumocephalus and Brain Shift**

7 Analysis of factors that may impact upon accuracy, specifically pneumocephalus and brain
8 shift, is presented in figure 6. Accuracy, in this instance defined as the mean accuracy across
9 hemispheres, positively correlated with brain shift, as defined by the total adjustment
10 performed by subcortical refine methodology, but this was not significant when corrected for
11 multiple comparisons ($r = 0.42$, $R^2 = 0.17$, $p = 0.022$). There was no correlation between
12 accuracy and pneumocephalus, nor between brain shift and pneumocephalus.

13

14 **Accuracy and Clinical Outcomes**

15 Finally, the relationship of accuracy to clinical outcomes is presented in supplementary
16 figures 5 and 6. Note that for GPi stimulation there were insufficient outcome data available
17 for analysis and these data were excluded, hence these analyses are exclusively for STN
18 stimulation. The VAT in either the main nucleus or motor sub-nucleus did not correlate with
19 clinical outcomes. Furthermore, overall electrode accuracy did not correlate with the VAT in
20 either the main nucleus or the motor nucleus ($r = -0.19$, $p = 0.43$).

21

22 **DISCUSSION**

23

24 In summary, we performed a systematic appraisal of DBS electrode accuracy using
25 contemporary neuroimaging methods. Overall, accuracy was high. However, accuracy was

1 lower in the GPi than STN, and for the second electrode implanted. This inaccuracy was
2 found to occur predominantly in the X (lateral) dimension. Neither brain shift nor
3 pneumocephalus were found to be associated with lower accuracy. Finally, electrode
4 accuracy did not impact upon the total VAT able to be generated, nor on any one specific
5 clinical outcome.

6

7 Lower accuracy in the second electrode implantation is a well-known issue. Risk factors
8 include cerebral atrophy [29]. Recognised methods to address this include adding a specific
9 offset to the final frame co-ordinates [29] and performing staged surgery. It could also be
10 argued that awake surgery with macrostimulation or microelectrode recordings, potentially
11 with multiple tracts, would allow feedback of the ideal location. Other proposals include
12 continuous irrigation after durotomy to minimise brain shift and pneumocephalus. Device
13 hardware developments, for example local field potential recording of the best target or using
14 directional stimulation, may facilitate compensation for lower accuracy. Nevertheless, with
15 the lack of correspondence between accuracy and clinical outcomes or the VAT that was able
16 to be generated, it would appear wise to not attempt elaborate methods of compensation for
17 what in practice is apparently satisfactory accuracy.

18

19 Historically, accuracy has been appraised by comparing electrode implantations with that
20 planned, typically using AC-PC co-ordinates. However, few consistent factors have emerged
21 to guide improved accuracy. Furthermore, this method does not easily facilitate group
22 analysis of multiple electrodes, comparison with functional templates (e.g. to delineate the
23 motor subnucleus), or appraise systematic variance in targeting (i.e. electrodes could be
24 precise and accurate but poorly planned within a nucleus). Our neuroimaging methodology
25 addresses these shortcomings and allows a systematic appraisal of electrode inaccuracy

1 accounting for both targeting and planning error. Using neuroimaging methods, we were able
2 to not only identify the specific clinical situations where accuracy was lower, but appraise
3 what factors were associated with accuracy. Our findings suggest that brain shift and
4 pneumocephalus have less of an effect on accuracy than previously believed.

5
6 Nevertheless, a neuroimaging approach to accuracy should be seen as complimentary to
7 rather than superseding traditional co-ordinate approaches. Strengths of the traditional co-
8 ordinate approach include direct appraisal of how the final location compares to the intended
9 target and comparison with individual rather than template-based anatomy. It also allows for
10 a more clinically defined measure of accuracy in the order of millimetres from planned target,
11 rather than the somewhat lower distances involved using our definitions of accuracy.

12 However, when accuracy and clinical outlines are typically good, an extensive and detailed
13 database of outcomes is necessary to identify subtle features that may be associated with
14 accuracy in specific situations. For example, our sample size of $n=38$ would only be
15 sufficient for detecting an $r = 0.45$ with $\alpha = 0.05$ and $\beta = 0.20$ prior to multiple
16 comparisons corrections (<https://sample-size.net/correlation-sample-size>). With this in mind,
17 we have not appraised the effects of age or electrode type on accuracy, for example. Notably,
18 our methods lend themselves to easily performing these subsequent analyses, and we have
19 freely shared our code online to do so in the hope that other larger datasets will be able to test
20 these hypotheses in the future.

21
22 Establishing a ground truth with which to verify the accuracy of electrode localisation is an ill
23 posed problem without using post-mortem analysis[30]. Limitations in electrode localisation
24 include the difficulty in segmenting the STN automatically at the individual level, which even
25 with 7 Tesla MRI remains an evolving process[31]. Group templates have been introduced to

1 obviate this issue (as well as offering additional resolution and functional segmentation)[31].
2 However, it is unclear how well they reflect individual anatomy, particularly in the context of
3 a progressive neurodegenerative disease[32]. Other limitations of image processing pipelines
4 include those related to registration (which may be ameliorated to a degree by post-operative
5 MRI[33], and the utilisation of non-automated processes in electrode reconstruction (which
6 is currently easier with post-operative CT and may also potentially allow directionality
7 determination[20,34]. One must therefore be mindful that anatomical localisation data is only
8 one aspect in considering optimal electrode targeting and must be considered alongside the
9 complimentary neurophysiological and clinical parameters.

10

11 Overall, our accuracy was comparable with that presented in the literature, serving as a robust
12 audit of our method (specifically, general anaesthesia throughout, frame-based, direct
13 targeting, MRI-planned, and CT-verified)[6,7,11,35–39]. This accuracy is juxtaposed with
14 studies of microelectrode recordings have reported revision of the original imaging-based
15 targeting in approximately 20%. Despite this emphasis on accuracy, in our series electrode
16 localisation did not enable prediction of clinical outcomes, in contrast to that reported in the
17 literature[21,40,41]. One explanation for this could be a lack of statistical power related to
18 sample size and data attrition. Furthermore, when using VAT analysis, stimulation
19 parameters may not necessarily be optimal (due to either clinical factors or the multiple
20 permutations of programming parameters)[42], which may obfuscate any relationship
21 between accuracy and outcomes. Further work is required in exploring the relationship
22 between clinical outcomes, electrode location, and determining what is clinically meaningful
23 accuracy at the individual level.

24

1 Revision surgery has been documented as occurring in up to 15%[39,43–48] with consequent
2 effects on healthcare services, finances, and risk of surgical complications. Myriad
3 technologies have been proposed with the aim of improving accuracy, including the use of
4 robotics[49–52]. In our data we identified three participants each with a single electrode
5 location outside of the target nucleus by greater than 2mm. Reassuringly, this did not lead to
6 any adverse neurological outcomes or unsatisfactory treatment response – and therefore
7 neither electrode was revised – but nor was there a clear clinical indication of why
8 discrepancy from the usual accuracy occurred. Overall, these data suggest that the accuracy
9 achieved in routine practice is sufficient to not adversely impact upon clinical outcomes
10
11 Strengths of our study include the implementation of a relatively lightweight design and
12 analysis strategy that integrates efficiently with a busy clinical movement disorders practice.
13 Furthermore, we have released detailed open-source code to make this process more
14 accessible. Limitations include the overall numbers and attrition, although these data
15 represent a realistic reflection of what can be achieved in routine clinical practice.
16 Improvements include focusing on streamlining data collection and optimising imaging
17 parameters. However, the main factor that will play into improving study power will be the
18 establishment of multi-centre collaborations and open-source datasets.
19
20 Emergence of open-source lead localisation software compliments an overall burgeoning in
21 DBS hardware and research. Accurate appraisal of lead localisation is not only useful in deep
22 brain stimulation surgery, but also in lesioning, cell delivery studies, and stereo-
23 electroencephalography (SEEG). Furthermore, lead localisation can be used to appraise
24 changes to clinical practice (such as a change in imaging sequences, surgical workflow, or
25 head position), which can now be objectively audited. This work therefore represents an ideal

1 platform for large multi-centre audits and specifically trainee projects[53]. Such research,
2 when performed systematically and with sufficient statistical power, may go some way to
3 improving our understanding of accuracy and precision, as well as deriving optimal surgical
4 workflows.

5

6 **CONCLUSIONS**

7 In conclusion, our analysis is supportive of the accuracy in performing deep brain stimulation
8 in a fully image-guided manner under general anaesthesia, but highlights the complexity of
9 understanding accuracy, and cautions about lower accuracy during the second electrode. We
10 hope that publication of these data and resources will encourage groups to utilise
11 developments in electrode localisation, develop collaborations, and provide large open-source
12 datasets that enhance our understanding of outcomes after deep brain stimulation.

13

14 **ACKNOWLEDGEMENTS**

15 The authors report no acknowledgements.

16

17

18 **FIGURE LEGENDS**

19

20 **Figure 1: Image Processing Pipeline**

21 A: Post-operative CT scans were linearly registered to the pre-operative MRI which in turn
22 was registered to the standard space of the Montreal Neurological Institute using non-linear
23 diffeomorphic warping. Subsequently, subcortical structures were subject to an additional
24 rigid registration to account for brain shift (subcortical refine). Both transforms were
25 combined and applied. Electrode reconstruction was performed using either PaCER for non-

1 directional leads or TRA/CORE for directional leads. Subsequently a Volume of Activated
2 Tissue (VAT) was generated as a mesh and displayed on a template atlas. B: electrode
3 distances were defined according to distance from nucleus border (right) for analysis of
4 accuracy, or distance to either the main nucleus (grey asterisk) or motor subnucleus (white
5 asterisk) when analysing XYZ variance.

6

7 **Figure 2: Clinical Outcomes**

8 Raincloud plots of changes in the five clinical outcome variables. Upper rows (green) are pre-
9 operative values, lower rows (orange) are post-operative scores. All changes are as
10 percentages. t_{stat} = paired t-test value. Raincloud plots display the raw data, box plots, and
11 half-violin plots of the data distribution ([28]).

12

13 **Figure 3: Electrode Accuracy Summary**

14 I: Overall accuracy for all electrodes for both targets (GPi and STN) and hemispheres (60
15 electrodes). In total 9 outliers were identified and only 3 electrodes out with 2mm from the
16 intended target. II: Electrodes implanted in the GPi had lower accuracy than those implanted
17 in the STN. III: Electrode accuracy did not systemically vary between sides (i.e. it was not
18 the case that low accuracy in one hemisphere was associated with low in the other
19 hemisphere, related to for example a shared methodological step). IV: Electrode accuracy
20 varied between hemispheres with reduced accuracy in the right hemisphere which was the
21 second side implanted.

22

23 **Figure 4: Group Electrode Location Visualisation**

24 A: subthalamic nucleus electrode reconstructions B: corresponding subthalamic nucleus
25 electrode contacts on the right (upper) and left (lower). C: globus pallidus internus electrode

1 reconstructions D: corresponding globus pallidus interna electrode contacts on the right
2 (upper) and left (lower). The background image for all figures is from the BigBrain project
3 (<https://bigbrain.loris.ca/main.php?>) under CC-BY-NC-SA 4.0 license.

4

5 **Figure 5: Target Plots of Electrode Location**

6 Electrode co-ordinates are displayed in relation to the target centre of gravity (see figure 1B
7 left). This allows systematic visual inspection of lateral (X) and anterior (Y) plane variance
8 viz a viz accuracy and precision of group targeting. These plots are systematically arranged
9 per target (STN: upper two rows, GPi: lower two rows), nucleus (main: left two columns,
10 motor: right two columns), and hemisphere. Rows two and four remove the subcortical refine
11 (nSCRF) that compensates for brain shift from the corresponding co-ordinates in the row
12 above.

13

14 **Figure 6: Accuracy, Pneumocephalus, and Brain Shift**

15 Electrode accuracy and averaged across hemispheres. Brain shift is reflected in the summed
16 total of the subcortical refine (SCRF) transformation matrix. Pneumocephalus is assessed
17 using a standard space brain mask (figure 1C). Increased brain shift, reflected in higher SCRF
18 values, is correlated with reduced accuracy. However, accuracy is not correlated with brain
19 shift, and brain shift is not correlated with pneumocephalus.

20

21 **Supplementary Figure 1: Study Flow Chart**

22 Flow chart of study recruitment and data attrition.

23

24 **Supplementary Figure 2: Clinical Outcomes Plotmatrix**

1 Plotmatrix of changes in the five clinical outcome variables. Spearman's rank correlation
2 coefficient (r_s) with associated p -values between outcome pairs are presented in the upper
3 triangle while raw datapoints are presented in the corresponding lower triangle. The diagonal
4 represents differences in outcomes depending on target location (GPi or STN) with
5 corresponding unpaired t -. GPi: Globus Pallidus Internus, LEDD: levodopa equivalent daily
6 dose, PDQ39: Parkinson's Disease Questionnaire, STN: Subthalamic nucleus, UPDRS:
7 Unified Parkinson's Disease Rating Scale

8

9 **Supplementary Figure 3: Systematic Appraisal of Electrode Accuracy and Clinical** 10 **Scenarios**

11 I: Accuracy was not systematically different when appraised either based on the main nucleus
12 or motor subnucleus centre of gravity (figure 1C, left). II: Accuracy in the motor nucleus did
13 not vary across hemispheres in the STN but did in the GP (III). A similar pattern was
14 identified in the motor subnucleus with accuracy not varying across hemispheres in the STN
15 (IV) but did in the GPi (V).

16

17 **Supplementary Figure 4: Systematic Appraisal of XYZ Variance in Targeting**

18 Raincloud plots appraising systematic variance in individual XYZ planes. Variance was
19 identified across the group (group F -stat = 9.68, $df = 7$, $p < 0.01$) which reflected that in the X
20 dimension of the right GPi (GPi right single-group t -stat = -2.9, $df = 18$, $p = 0.01$). Distances
21 are from the target centre of gravity, in this case the motor subnucleus.

22

23 **Supplementary Figure 5: Volume of Activated Tissue (VAT) and Clinical Outcomes**

1 Statistical dependencies between VAT of the main nucleus (top row) and motor subnucleus
2 (lower row) with clinical outcomes (columns). No significant correlations or regression
3 models were identified.

4

5 **Supplementary Figure 6: Accuracy and Clinical Outcomes**

6 Statistical dependencies between electrode accuracy of the main nucleus (top row) and motor
7 subnucleus (lower row) with clinical outcomes (columns). No significant correlations or
8 regression models were identified.

9

10 **REFERENCES**

11

12 [1] Deuschl G, Schade-Brittinger C, Krack P, Volkmann J, Schäfer H, Bötzel K, et al. A
13 Randomized Trial of Deep-Brain Stimulation for Parkinson's Disease. *New Engl J Med*
14 2006;355:896–908. <https://doi.org/10.1056/nejmoa060281>.

15 [2] Weaver FM, Follett K, Stern M, Hur K, Harris C, Marks WJ, et al. Bilateral deep brain
16 stimulation vs best medical therapy for patients with advanced Parkinson disease: a
17 randomized controlled trial. *Jama* 2009;301:63–73. <https://doi.org/10.1001/jama.2008.929>.

18 [3] Williams A, Gill S, Varma T, Jenkinson C, Quinn N, Mitchell R, et al. Deep brain
19 stimulation plus best medical therapy versus best medical therapy alone for advanced
20 Parkinson's disease (PD SURG trial): a randomised, open-label trial. *Lancet Neurology*
21 2010;9:581–91. [https://doi.org/10.1016/s1474-4422\(10\)70093-4](https://doi.org/10.1016/s1474-4422(10)70093-4).

22 [4] Okun MS. Deep-brain stimulation for Parkinson's disease. *The New England Journal of*
23 *Medicine* 2012;367:1529–38. <https://doi.org/10.1056/nejmct1208070>.

24 [5] Schuepbach WMM, Rau J, Knudsen K, Volkmann J, Krack P, Timmermann L, et al.
25 Neurostimulation for Parkinson's Disease with Early Motor Complications. *New Engl J*
26 *Medicine* 2013;368:610–22. <https://doi.org/10.1056/nejmoa1205158>.

27 [6] Saint-Cyr JA, Hoque T, Pereira LCM, Dostrovsky JO, Hutchison WD, Mikulis DJ, et al.
28 Localization of clinically effective stimulating electrodes in the human subthalamic nucleus
29 on magnetic resonance imaging. *J Neurosurg* 2002;97:1152–66.
30 <https://doi.org/10.3171/jns.2002.97.5.1152>.

31 [7] McClelland S, Ford B, Senatus PB, Winfield LM, Du YE, Pullman SL, et al. Subthalamic
32 stimulation for Parkinson disease: determination of electrode location necessary for clinical
33 efficacy. *Neurosurg Focus* 2005;19:1–9. <https://doi.org/10.3171/foc.2005.19.5.13>.

- 1 [8] III SM, Vonsattel JP, Garcia RE, Amaya MD, Winfield LM, Pullman SL, et al.
2 Relationship of clinical efficacy to postmortem-determined anatomic subthalamic stimulation
3 in Parkinson syndrome. *Clin Neuropathol* 2007;26:267–75.
4 <https://doi.org/10.5414/npp26267>.
- 5 [9] Pilitsis JG, Metman LV, Toleikis JR, Hughes LE, Sani SB, Bakay RAE. Factors involved
6 in long-term efficacy of deep brain stimulation of the thalamus for essential tremor. *J*
7 *Neurosurg* 2008;109:640–6. <https://doi.org/10.3171/jns/2008/109/10/0640>.
- 8 [10] Bari AA, Thum J, Babayan D, Lozano AM. Current and Expected Advances in Deep
9 Brain Stimulation for Movement Disorders. *Prog Neurol* 2018;33:222–9.
10 <https://doi.org/10.1159/000481106>.
- 11 [11] Burchiel KJ, McCartney S, Lee A, Raslan AM. Accuracy of deep brain stimulation
12 electrode placement using intraoperative computed tomography without microelectrode
13 recording. *J Neurosurg* 2013;119:301–6. <https://doi.org/10.3171/2013.4.jns122324>.
- 14 [12] Chen T, Mirzadeh Z, Ponce FA. “Asleep” Deep Brain Stimulation Surgery: A Critical
15 Review of the Literature. *World Neurosurg* 2017;105:191–8.
16 <https://doi.org/10.1016/j.wneu.2017.05.042>.
- 17 [13] Ho AL, Ali R, Connolly ID, Henderson JM, Dhall R, Stein SC, et al. Awake versus
18 asleep deep brain stimulation for Parkinson’s disease: a critical comparison and meta-
19 analysis. *J Neurology Neurosurg Psychiatry* 2018;89:687. [https://doi.org/10.1136/jnnp-2016-](https://doi.org/10.1136/jnnp-2016-314500)
20 [314500](https://doi.org/10.1136/jnnp-2016-314500).
- 21 [14] Ko AL, Burchiel KJ. Image-Guided, Asleep Deep Brain Stimulation. *Prog Neurol*
22 2018;33:94–106. <https://doi.org/10.1159/000480984>.
- 23 [15] Miocinovic S, Noecker AM, Maks CB, Butson CR, McIntyre CC. *Acta Neurochirurgica*
24 *Supplements*. *Acta Neurochir Suppl* 2007;97:561–7. [https://doi.org/10.1007/978-3-211-](https://doi.org/10.1007/978-3-211-33081-4_65)
25 [33081-4_65](https://doi.org/10.1007/978-3-211-33081-4_65).
- 26 [16] D’Albis T, Haegelen C, Essert C, Fernández-Vidal S, Lalys F, Jannin P. PyDBS: an
27 automated image processing workflow for deep brain stimulation surgery. *Int J Comput Ass*
28 *Rad* 2015;10:117–28. <https://doi.org/10.1007/s11548-014-1007-y>.
- 29 [17] Horn A, Kühn AA. Lead-DBS: A toolbox for deep brain stimulation electrode
30 localizations and visualizations. *Neuroimage* 2015;107:127–35.
31 <https://doi.org/10.1016/j.neuroimage.2014.12.002>.
- 32 [18] Silva NM da, Rozanski VE, Cunha JPS. A 3D multimodal approach to precisely locate
33 DBS electrodes in the basal ganglia brain region. 2015 7th Int Ieee Embs Conf Neural Eng
34 *Ner* 2015:292–5. <https://doi.org/10.1109/ner.2015.7146617>.
- 35 [19] Lauro PM, Vanegas- Arroyave N, Huang L, Taylor PA, Zaghoul KA, Lungu C, et al.
36 DBSproc: An open source process for DBS electrode localization and tractographic analysis.
37 *Hum Brain Mapp* 2016;37:422–33. <https://doi.org/10.1002/hbm.23039>.

- 1 [20] Husch A, Petersen MV, Gemmar P, Goncalves J, Hertel F. PaCER - A fully automated
2 method for electrode trajectory and contact reconstruction in deep brain stimulation. YNICL
3 2018;17:80–9. <https://doi.org/10.1016/j.nicl.2017.10.004>.
- 4 [21] Horn A, Li N, Dembek TA, Kappel A, Boulay C, Ewert S, et al. Lead-DBS v2: Towards
5 a comprehensive pipeline for deep brain stimulation imaging. *NeuroImage* 2019;184:293–
6 316. <https://doi.org/10.1016/j.neuroimage.2018.08.068>.
- 7 [22] Board NC. Clinical Commissioning Policy: Deep Brain Stimulation (DBS) In
8 Movement Disorders. 2013.
- 9 [23] (NICE) NI for H and CE. NICE Guidelines NG71: Parkinson’s disease in adults:
10 diagnosis and management. NICE; 2017.
- 11 [24] Avants BB, Avants B, Tustison N, Johnson H, Yushkevich P. Advanced Normalization
12 Tools: V1. 0. Insight ...; 2009.
- 13 [25] Tustison NJ, Avants BB, Cook PA. The ANTs cortical thickness processing pipeline.
14 *SPIE Medical ...* 2013;8672:86720K – 2. <https://doi.org/10.1117/12.2007128>.
- 15 [26] Schönecker T, Kupsch A, Kühn AA, Schneider G-H, Hoffmann K-T. Automated
16 Optimization of Subcortical Cerebral MR Imaging–Atlas Coregistration for Improved
17 Postoperative Electrode Localization in Deep Brain Stimulation. *Am J Neuroradiol*
18 2009;30:1914–21. <https://doi.org/10.3174/ajnr.a1741>.
- 19 [27] Ewert S, Plettig P, Li N, Chakravarty MM, Collins DL, Herrington TM, et al. Toward
20 defining deep brain stimulation targets in MNI space: A subcortical atlas based on
21 multimodal MRI, histology and structural connectivity. *Neuroimage* 2018;170:271–82.
22 <https://doi.org/10.1016/j.neuroimage.2017.05.015>.
- 23 [28] Allen M, Poggiali D, Whitaker K, Marshall TR, Kievit RA. Raincloud plots: a multi-
24 platform tool for robust data visualization. *Wellcome Open Res* 2019;4:63.
25 <https://doi.org/10.12688/wellcomeopenres.15191.1>.
- 26 [29] Park S-C, Lee JK, Kim SM, Choi EJ, Lee CS. Systematic Stereotactic Error Reduction
27 Using a Calibration Technique in Single-Brain-Pass and Multitrack Deep Brain Stimulations.
28 *Operative Neurosurg Hagerstown Md* 2018;15:72–80. <https://doi.org/10.1093/ons/oxp183>.
- 29 [30] Reddy GD, Lozano AM. Postmortem studies of deep brain stimulation for Parkinson’s
30 disease: a systematic review of the literature. *Cell Tissue Res* 2018;373:287–95.
31 <https://doi.org/10.1007/s00441-017-2672-2>.
- 32 [31] Visser E, Keuken MC, Forstmann BU, Jenkinson M. Automated segmentation of the
33 substantia nigra, subthalamic nucleus and red nucleus in 7T data at young and old age.
34 *Neuroimage* 2016;139:324–36. <https://doi.org/10.1016/j.neuroimage.2016.06.039>.
- 35 [32] Nowacki A, Nguyen TA-K, Tinkhauser G, Petermann K, Debove I, Wiest R, et al.
36 Accuracy of different three-dimensional subcortical human brain atlases for DBS –lead
37 localisation. *Neuroimage Clin* 2018;20:868–74. <https://doi.org/10.1016/j.nicl.2018.09.030>.

- 1 [33] Zrinzo L, Hariz M, Hyam JA, Foltynie T, Limousin P. Letter to the Editor: A paradigm
2 shift toward MRI-guided and MRI-verified DBS surgery. *J Neurosurg* 2016;124:1135–8.
3 <https://doi.org/10.3171/2015.9.jns152061>.
- 4 [34] Hellerbach A, Dembek TA, Hoevens M, Holz JA, Gierich A, Luyken K, et al. DiODE:
5 Directional Orientation Detection of Segmented Deep Brain Stimulation Leads: A Sequential
6 Algorithm Based on CT Imaging. *Stereot Funct Neuros* 2018;96:335–41.
7 <https://doi.org/10.1159/000494738>.
- 8 [35] Hamid NA, Mitchell RD, Mocoft P, Westby GWM, Milner J, Pall H. Targeting the
9 subthalamic nucleus for deep brain stimulation: technical approach and fusion of pre- and
10 postoperative MR images to define accuracy of lead placement. *Journal of Neurology,*
11 *Neurosurgery & Psychiatry* 2005;76:409–14. <https://doi.org/10.1136/jnnp.2003.032029>.
- 12 [36] Bjartmarz H, Rehncrona S. Comparison of accuracy and precision between frame-based
13 and frameless stereotactic navigation for deep brain stimulation electrode implantation.
14 *Stereotactic and Functional Neurosurgery* 2007;85:235–42.
15 <https://doi.org/10.1159/000103262>.
- 16 [37] Foltynie T, Zrinzo L, Martinez-Torres I, Tripoliti E, Petersen E, Holl E, et al. MRI-
17 guided STN DBS in Parkinson's disease without microelectrode recording: efficacy and
18 safety. *J Neurology Neurosurg Psychiatry* 2011;82:358.
19 <https://doi.org/10.1136/jnnp.2010.205542>.
- 20 [38] Ko AL, Ibrahim A, Magown P, Macallum R, Burchiel KJ. Factors Affecting Stereotactic
21 Accuracy in Image-Guided Deep Brain Stimulator Electrode Placement. *Stereotactic and*
22 *Functional Neurosurgery* 2017;95:315–24. <https://doi.org/10.1159/000479527>.
- 23 [39] Frizon LA, Nagel SJ, May FJ, Shao J, Maldonado-Naranjo AL, Fernandez HH, et al.
24 Outcomes following deep brain stimulation lead revision or reimplantation for Parkinson's
25 disease. *J Neurosurg* 2018:1–6. <https://doi.org/10.3171/2018.1.jns171660>.
- 26 [40] Bot M, Schuurman PR, Odekerken VJJ, Verhagen R, Contarino FM, Bie RMAD, et al.
27 Deep brain stimulation for Parkinson's disease: defining the optimal location within the
28 subthalamic nucleus. *J Neurology Neurosurg Psychiatry* 2018;89:493–8.
29 <https://doi.org/10.1136/jnnp-2017-316907>.
- 30 [41] Horn A, Wenzel G, Irmen F, Huebl J, Li N, Neumann W-J, et al. Deep brain stimulation
31 induced normalization of the human functional connectome in Parkinson's disease. *Brain*
32 2019;142:3129–43. <https://doi.org/10.1093/brain/awz239>.
- 33 [42] Koeglsperger T, Palleis C, Hell F, Mehrkens JH, Bötzel K. Deep Brain Stimulation
34 Programming for Movement Disorders: Current Concepts and Evidence-Based Strategies.
35 *Front Neurol* 2019;10:410. <https://doi.org/10.3389/fneur.2019.00410>.
- 36 [43] Ellis T-M, Foote KD, Fernandez HH, Sudhyadhom A, Rodriguez RL, Zeilman P, et al.
37 Reoperation for suboptimal outcomes after deep brain stimulation surgery. *Neurosurgery*
38 2008;63:754–61. <https://doi.org/10.1227/01.neu.0000325492.58799.35>.

- 1 [44] Falowski SM, Ooi YC, Bakay RAE. Long- Term Evaluation of Changes in Operative
2 Technique and Hardware- Related Complications With Deep Brain Stimulation.
3 Neuromodulation Technology Neural Interface 2015;18:670–7.
4 <https://doi.org/10.1111/ner.12335>.
- 5 [45] Patel DM, Walker HC, Brooks R, Omar N, Ditty B, Guthrie BL. Adverse events
6 associated with deep brain stimulation for movement disorders: analysis of 510 consecutive
7 cases. Neurosurgery 2015;11 Suppl 2:190–9.
8 <https://doi.org/10.1227/neu.0000000000000659>.
- 9 [46] Falowski SM, Bakay RAE. Revision Surgery of Deep Brain Stimulation Leads.
10 Neuromodulation Technology Neural Interface 2016;19:443–50.
11 <https://doi.org/10.1111/ner.12404>.
- 12 [47] Rolston JD, Englot DJ, Starr PA, Larson PS. An unexpectedly high rate of revisions and
13 removals in deep brain stimulation surgery: Analysis of multiple databases. Parkinsonism
14 Relat D 2016;33:72–7. <https://doi.org/10.1016/j.parkreldis.2016.09.014>.
- 15 [48] Nickl RC, Reich MM, Pozzi NG, Fricke P, Lange F, Roothans J, et al. Rescuing
16 Suboptimal Outcomes of Subthalamic Deep Brain Stimulation in Parkinson Disease by
17 Surgical Lead Revision. Neurosurgery 2019. <https://doi.org/10.1093/neuros/nyz018>.
- 18 [49] Xu F, Jin H, Yang X, Sun X, Wang Y, Xu M, et al. Improved accuracy using a modified
19 registration method of ROSA in deep brain stimulation surgery. Neurosurg Focus
20 2018;45:E18. <https://doi.org/10.3171/2018.4.focus1815>.
- 21 [50] Goia A, Gilard V, Lefaucheur R, Welter M, Maltête D, Derrey S. Accuracy of the
22 robot- assisted procedure in deep brain stimulation. Int J Medical Robotics Comput Assisted
23 Surg 2019;15. <https://doi.org/10.1002/rcs.2032>.
- 24 [51] Liu L, Mariani SG, Schlichting ED, Grand S, Lefranc M, Seigneuret E, et al. Frameless
25 ROSA® Robot-Assisted Lead Implantation for Deep Brain Stimulation: Technique and
26 Accuracy. Oper Neurosurg 2019. <https://doi.org/10.1093/ons/opz320>.
- 27 [52] VanSickle D, Volk V, Freeman P, Henry J, Baldwin M, Fitzpatrick CK. Electrode
28 Placement Accuracy in Robot-Assisted Asleep Deep Brain Stimulation. Ann Biomed Eng
29 2019;47:1212–22. <https://doi.org/10.1007/s10439-019-02230-3>.
- 30 [53] Chari A, Jamjoom AA, Edlmann E, Ahmed AI, Coulter IC, Ma R, et al. The British
31 Neurosurgical Trainee Research Collaborative: Five years on. Acta Neurochir 2017;160:23–
32 8. <https://doi.org/10.1007/s00701-017-3351-5>.

33

Table 1. Cohort Baseline Clinical and Demographic Data

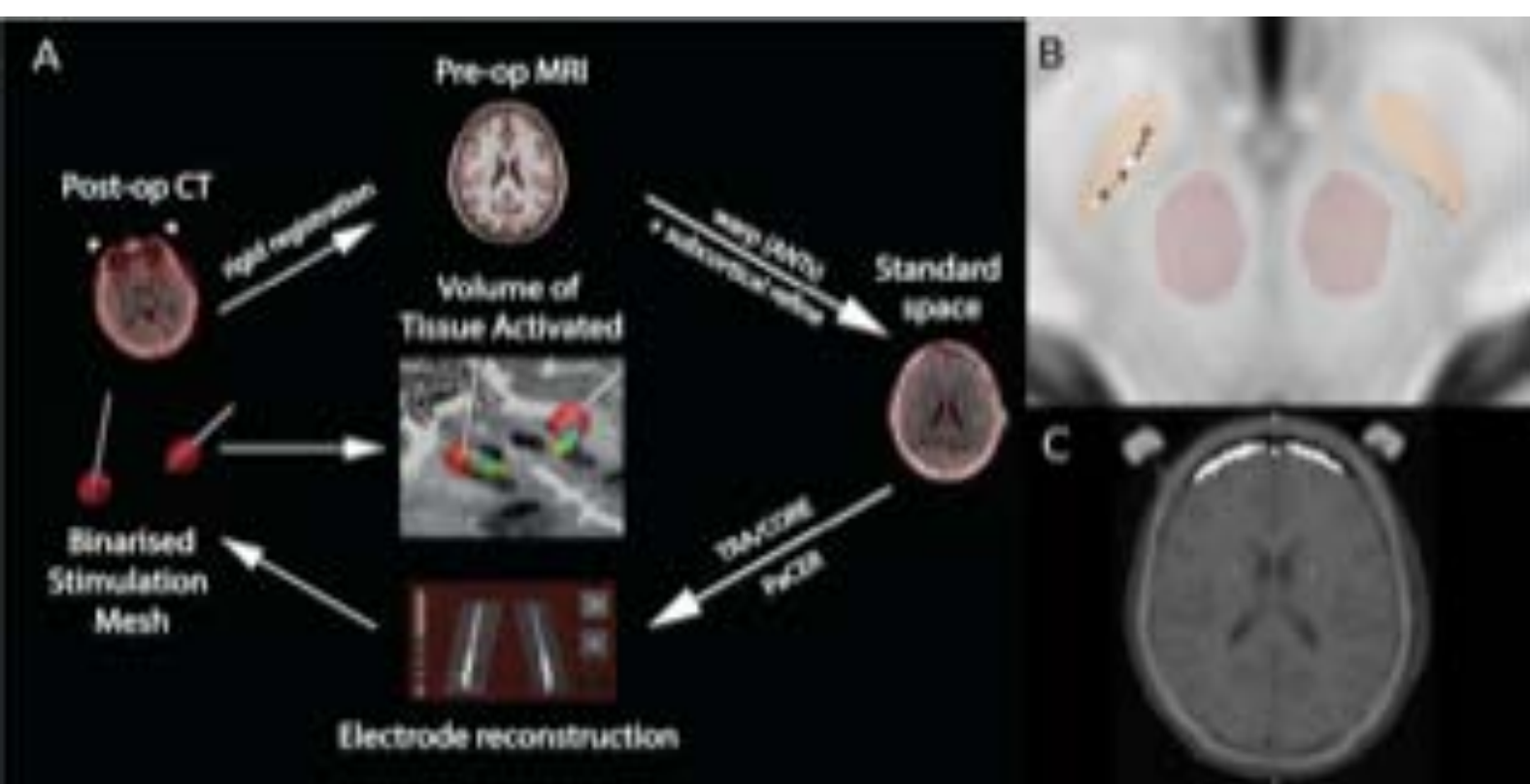
Feature		Value
Gender	Female	14
	Male	24
Age		62.1 (7.8)
Disease duration		11.8 (6.7)
Target	GPI	15
	STN	23
Manufacturer	Abbott / St Jude	28
	Boston Scientific	7
	Medtronic	3
UPDRS 3		48.1 (9.5)
UPDRS 4		8.6 (4.4)
LEDD		1112.8 (575.3)
PDQ39		76.5 (22.5)
MOCA		25.8 (4.1)

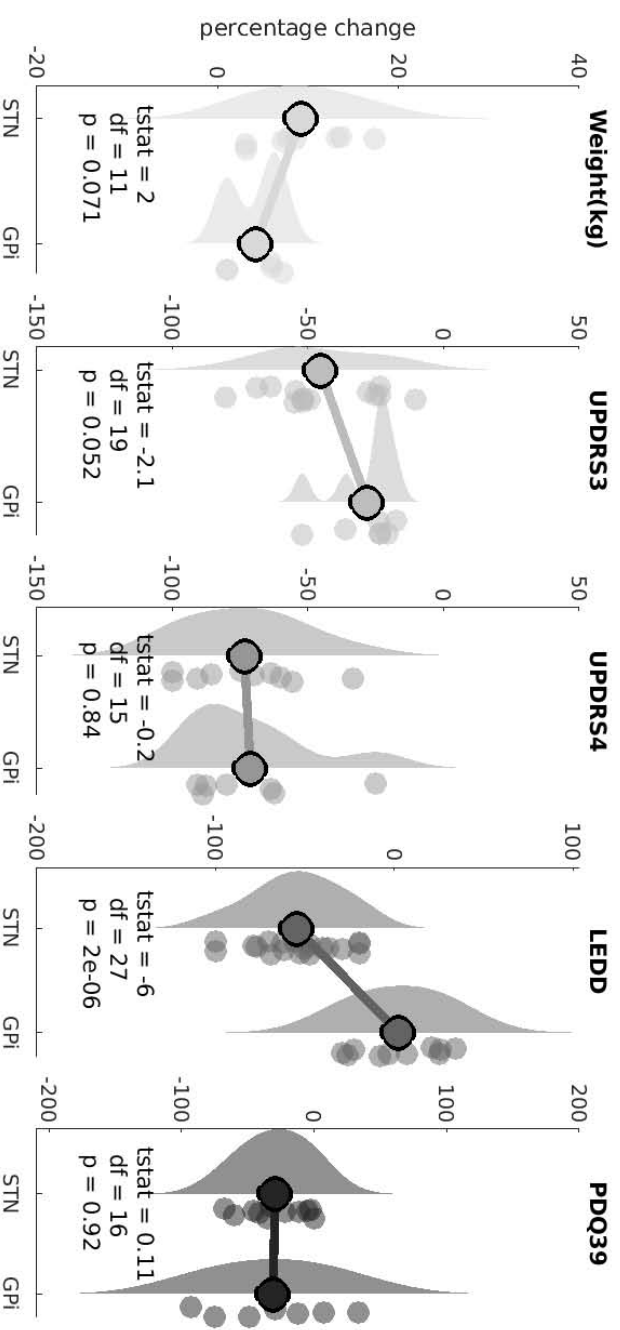
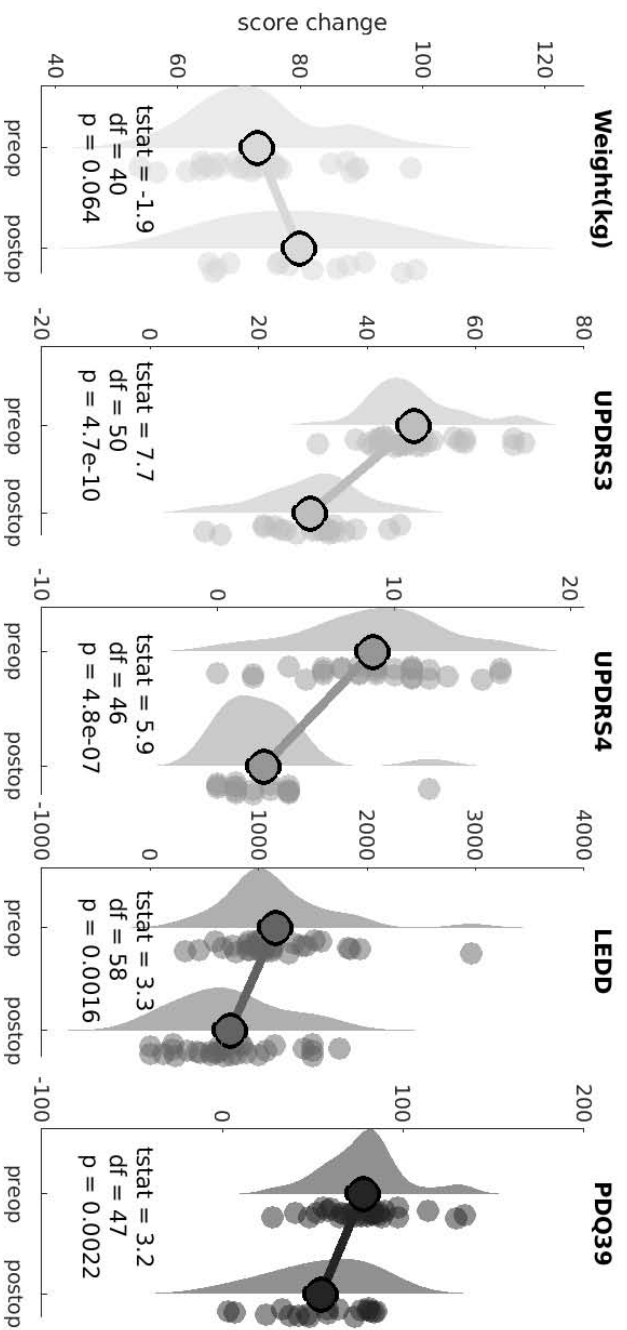
All results for UPDRS are off medication. Continuous measures are mean (+/- 2 standard deviation). Time data is in years. Levodopa equivalent daily dose (LEDD) is in mg.

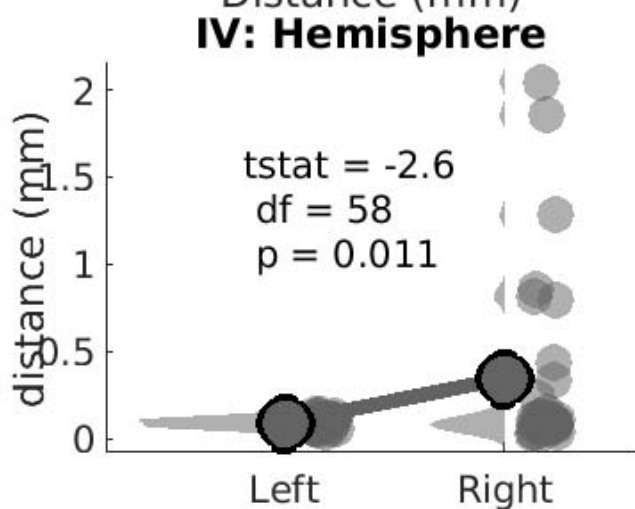
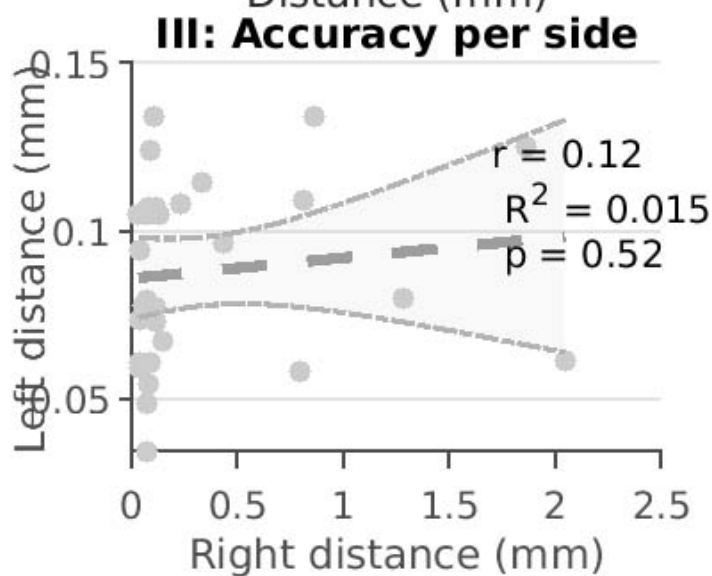
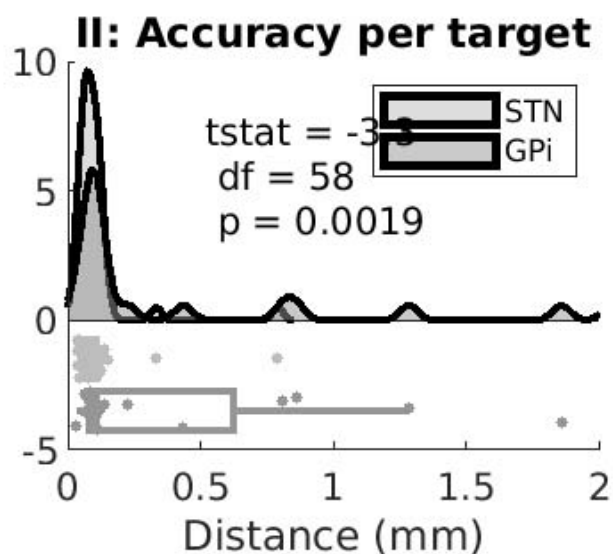
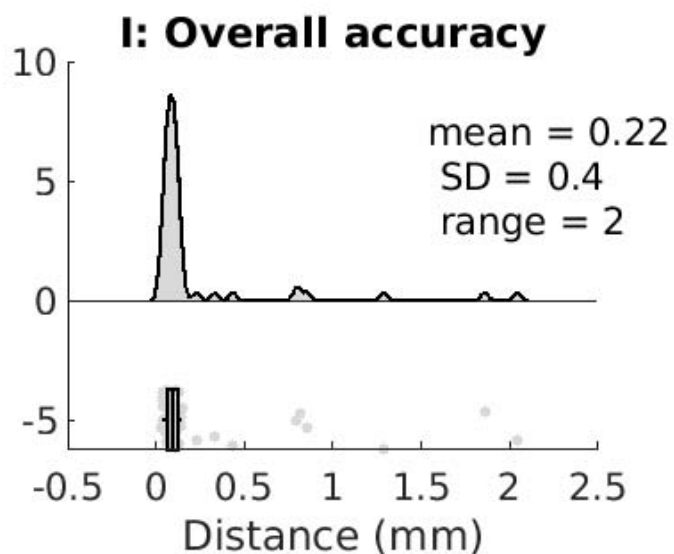
Table 2. Clinical outcomes

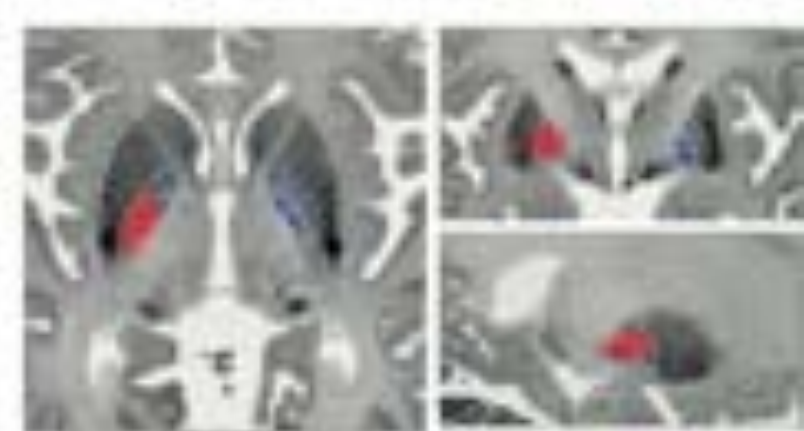
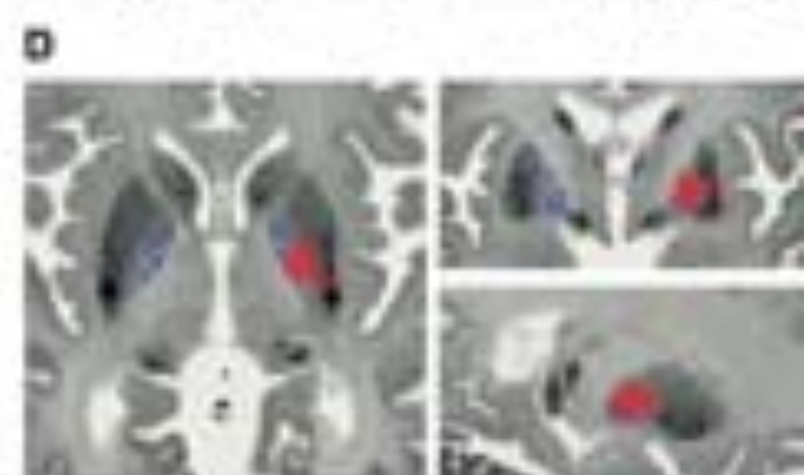
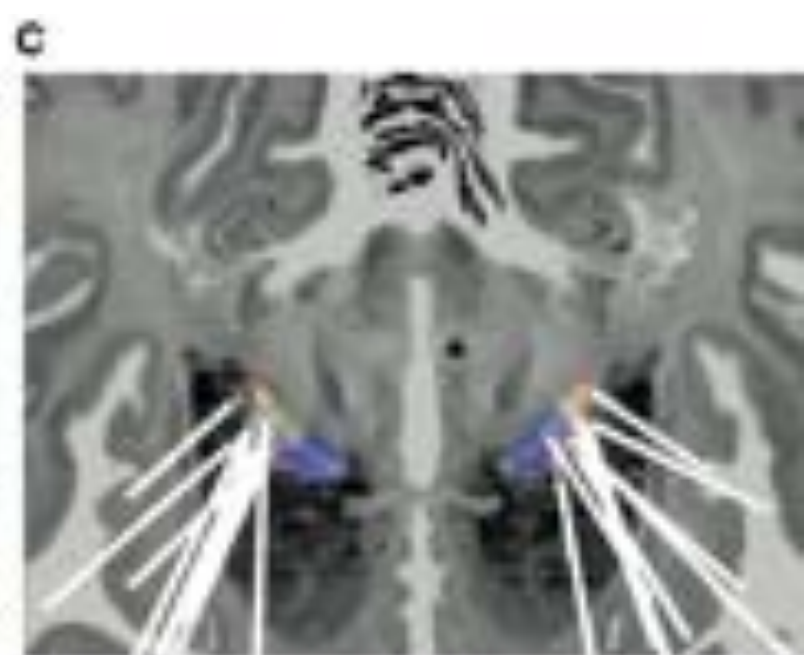
	Overall	Target		Gender	
		GPi	STN	Female	Male
UPDRS 3	-45.9%	-30.5%	-51.8%	-32.9%	-54.2%
	(23.5)	(13.8)	(24.1)	(13.3)	(25.2)
UPDRS 4	-72.2%	-76.5%	-70.1%	-77.0%	-69.8%
	(23.5)	(12.7)	(44.7)	(16.9)	(44.0)
LEDD	-35.9%	0.9%	-54.3%	-27.6%	-41.8%
	(36.1)	(25.1)	(24.9)	(33.2)	(38.1)
PDQ39	-32.1%	-31.1%	-32.6%	-31.5%	-32.5%
	(34.6)	(53.3)	(24.4)	(31.9)	(38.1)
Weight	8.7%	5.0%	10.8%	10.6%	9.0%
	(5.4)	(2.7)	(5.6)	(5.9)	(5.5)

Motor scores are off medication. Continuous measures are mean (+/- 2 standard deviations). Time data is in years. LEDD is in mg.

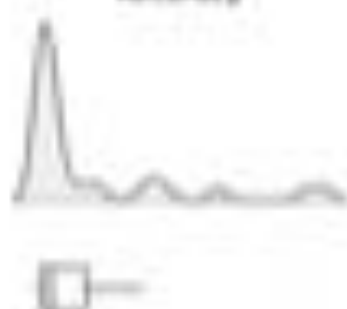








Accuracy

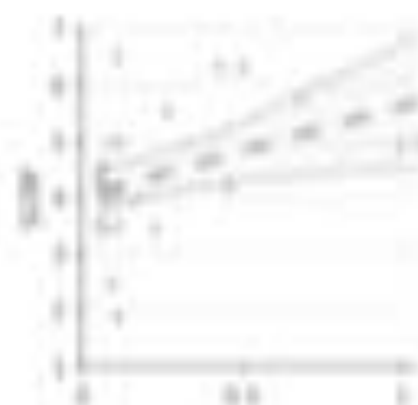


GCMS

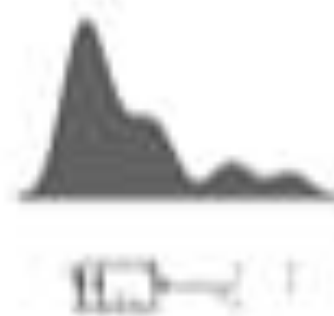
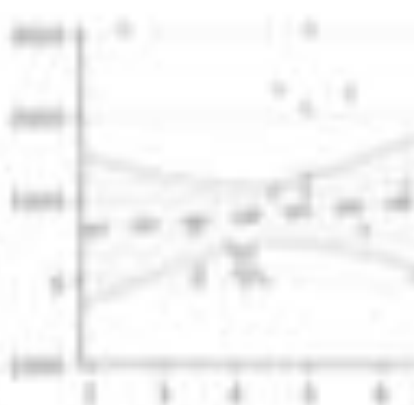
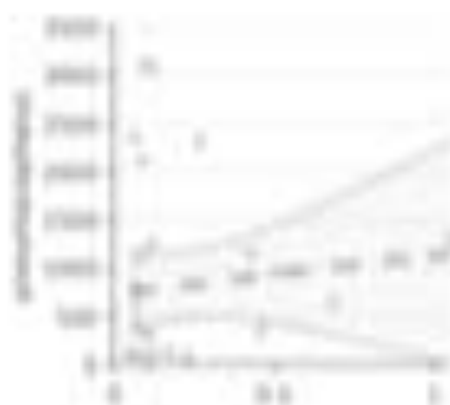
$r = 0.92$
 $R^2 = 0.85$
 $p < 0.001$

Pneumococcal

$r = 0.85$
 $R^2 = 0.72$
 $p < 0.001$



$r = 0.88$
 $R^2 = 0.78$
 $p < 0.001$



Highlights

- Overall electrode accuracy was $0.22 \pm 0.4\text{mm}$ with only 3 (4%) electrodes out with 2mm from the intended target
- Accuracy was significantly worse in the GPi versus the STN and on the second side implanted
- Inaccuracy occurred in the X (lateral) plane but was not related to pneumocephalus or brain shift

Declaration of interests

The authors declare that they have no known competing financial interests or personal relationships that could have appeared to influence the work reported in this paper.

The authors declare the following financial interests/personal relationships which may be considered as potential competing interests:

Journal Pre-proof